

## Self-similarity and coarsening rate of a convecting bicontinuous phase separating mixture: Effect of the viscosity contrast

Hervé Henry<sup>1</sup> and György Tegze<sup>2</sup>

<sup>1</sup>Laboratoire de Physique de la Matière Condensée, École Polytechnique, CNRS, Université Paris-Saclay, F-91128 Palaiseau Cedex, France

<sup>2</sup>Wigner Research Centre for Physics, P.O. Box 49, H-1525 Budapest, Hungary



(Received 5 May 2017; revised manuscript received 29 August 2017; published 30 July 2018)

We present a computational study of the hydrodynamic coarsening in three dimensions of a critical mixture using the Cahn-Hilliard/Navier-Stokes model. The topology of the resulting intricate bicontinuous microstructure is analyzed through the principal curvatures to prove self-similar morphological evolution. We find that the self-similarity exists for both systems: isoviscous and with variable viscosity. However, the two systems have a distinct topological character. Moreover, an effective viscosity that accurately predicts the coarsening rate is proposed.

DOI: [10.1103/PhysRevFluids.3.074306](https://doi.org/10.1103/PhysRevFluids.3.074306)

### I. INTRODUCTION

Among the physical processes leading to the formation of a microstructure, phase separation is ubiquitous. It is seen in glasses [1] and polymer blends [2], and can be divided into two stages. First, the unstable mixture phase separates at a characteristic length scale  $l$  [3]. When the volume fraction of one phase is close to 0.5, the initial microstructure that arises consists of two interlaced percolating clusters (similar to the one presented in Fig. 1), while for significantly lower volume fractions it consists of isolated droplets in a matrix of the majority phase. This pattern evolves under the effect of diffusion [4] or of fluid flow [5], resulting in an increase of the characteristic length  $l$  known as coarsening. It is widely acknowledged that this process is self-similar. In the case of diffusive coarsening, based either on analytical [4] or numerical investigations [6,7], strong arguments in favor of this hypothesis can be found.

In the case of viscous coarsening, such arguments are still lacking. Indeed, Siggia [5], assuming *a priori* self-similarity, proposed using a scaling argument, that after an initial diffusive coarsening stage where the characteristic length grows as  $t^{1/3}$ , coarsening is governed by viscous fluid flow. This later regime is characterized by a growth of the characteristic length at a constant rate. Later, some consequences of self-similarity were observed in experiments [8,9] and numerical simulations [10–12] that were conducted at a symmetric composition where phases share the same viscosity. In further investigations, laws that account for inertial effects were also proposed [13–17]. However, these were limited to the symmetric case, and the existence of the viscous self-similar coarsening regime remains to be uncovered when the symmetry of the composition, or the kinetics, is broken. Moreover, the method of analysis was based on analyzing the structure functions, that is, losing accuracy at low wave numbers, and, more importantly, it gives no direct information about the topology of the microstructure.

Herein, inspired by recent x-ray tomography [18,19] experiments, we explore the effect of viscosity contrast of the phases on the persistence of self-similarity and the topology of the interconnected structure. Our analysis is based on simulations using the Cahn-Hilliard/Navier-Stokes (NSCH) model, and characterizes the geometrical features of the microstructure using recent advanced methods [6,20]

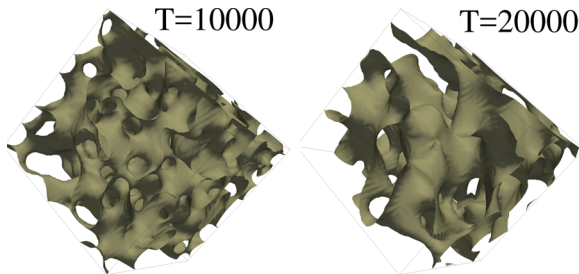


FIG. 1. Perspective view of the isosurface  $c = 0.5$  at different times of a simulation. The volume fraction is  $\varphi = 0.5$ , the viscosity contrast between the phases is 128, and the viscosity is  $\nu = 2$ .

We first study the hydrodynamic coarsening of an iso-viscous sample as a reference, and discuss the domain of validity of Siggia's scaling. Next, the effects of kinetic symmetry breaking (viscosity contrast) are considered and quantitative measures to the changes of the microstructure are given.

## II. THEORY AND MODELING

The thermodynamics of a binary fluid is well described by the diffuse interface theory of Cahn and Hilliard [21]. The simplest symmetric form of the Cahn-Hilliard free-energy reads as

$$\mathcal{F} = \int \epsilon^2 (\nabla c)^2 + A(c^2(c-1)^2). \quad (1)$$

Here,  $\epsilon$  and  $A$  are model parameters that are used to adjust the interface tension to  $\gamma = 0.0042$  as in Ref. [12]. The coarsening dynamics via convection and diffusion is governed by the coupled Navier-Stokes [Eq. (4)] and the convective Cahn-Hilliard (CH) [Eq. (2)] equations (NSCH), also known as model H [22]. Thermal fluctuations were neglected, assuming they are small on the characteristic scale of the microstructure. The Navier-Stokes/Cahn-Hilliard [23] model was used along with the incompressibility constraint [Eq. (4)],

$$\partial_t c + \mathbf{v} \cdot \nabla c = -D \Delta \mu, \quad (2)$$

$$\partial_t \mathbf{v} + \nabla \cdot (\mathbf{v} \otimes \mathbf{v}) = \frac{-1}{\rho} (\nabla p + c \nabla \mu) + \nabla \cdot \left( \frac{\nu(c)}{2} (\nabla \mathbf{v} + \nabla \mathbf{v}^T) \right), \quad (3)$$

$$\nabla \cdot \mathbf{v} = 0. \quad (4)$$

In the Cahn-Hilliard equation [Eq. (2)],  $D$  is the diffusion constant, and  $\mu = \delta \mathcal{F} / \delta c$  is the chemical potential that derives from the CH free energy.

In the Navier-Stokes equation [Eq. (3)] the  $-\nabla p$  term on the right-hand side (RHS) includes a Lagrangian multiplier that forces incompressibility. The second term is the thermodynamic stress, and accounts for capillary forces. The last term accounts for the viscous dissipation, and  $\nu(c) = \nu_h(1-c) + \nu_l(c)$  is the composition-dependent kinematic viscosity.  $\rho$  is the mass density and was chosen to unity unless otherwise specified. We define here the viscosity contrast as the ratio of the high and low viscosity of the species ( $VC = \nu_h/\nu_l$ ). While, according to the Stokes-Einstein relation, varying viscosity implies concentration-dependent diffusivity, in the late stage of coarsening one can assume local equilibrium at the interface. Therefore, simplifying to a homogeneous diffusion equation does not affect the coarsening of the microstructure. In addition, the absence of viscoelastic terms is valid under the assumption that the shear modulus is sufficiently high [24]. The model equations were simulated numerically using standard approaches [25–28] that are described in the Supplemental Material [29], together with a more detailed description of the model equations that are inspired by Refs. [30,31]. The analysis of the results allowed us to extract a characteristic length

scale  $l$  that is defined as the ratio between the total volume and the total interface between the phases and other statistical quantities such as the probability distribution function of the curvatures of the interface [32] or the structure functions. A detailed description of the method used to compute such quantities is also given in the Supplemental Material [29].

The NSCH model reproduces well the initial phase separation followed by the coarsening of the microstructure that is due to diffusion at small length scales with a characteristic length scale growing as  $l \propto t^{1/3}$  [4,33]. At larger length scales the coarsening is driven by convection that is governed by surface tension and viscous dissipation. As a result,  $l$  grows linearly,  $l = v_0 t \propto \gamma/vt$  [5], where  $\gamma$  is the surface tension and  $v$  is the viscosity of the fluid when  $VC = 1$ . The transition from the diffusive growth to a viscous growth occurs when  $v_0$  is much larger than the growth velocity associated with diffusion (which itself is a function of the mobility of chemical species). This translates into the fact that the Peclet number ( $Pe = lv_0/D$ ) is large. Finally, the viscous growth law loses its validity when inertial effects cannot be neglected [the Reynolds number  $Re$ , defined as  $l/l_0$ , where  $l_0 = v^2/(\gamma\rho)$  becomes large]. Here, we have limited ourselves to the viscous coarsening of a phase separated mixture, assuming that the viscosity was sufficiently high to avoid the effects of fluid flow during the initial phase separation and before well-defined phases are present and coarsening takes place [34]. It is important to note that during the course of the coarsening, since  $l$  is growing, these two numbers grow (proportionally to  $l$ ). This indicates that the characteristic size of the flow is the characteristic size of the microstructure and change with times. As a result, during the coarsening of a bicontinuous structure, both  $l$  and  $Re$  will increase and there will be a transition from a diffusive coarsening regime where  $Pe \ll 1$  to a viscous dominated regime ( $Pe \gg 1$  and  $Re \ll 1$ ), followed by an inertia dominated regime ( $Re \gg 1$ ) [35]. Here, we have focused on the well-defined Siggia regime for which  $Pe \gg 1$  and  $Re \ll 1$ .

### III. RESULTS

Since we consider the effect of the symmetry breaking induced by the viscosity contrast on the viscous coarsening, we have chosen to limit ourselves to the case where the volume fraction of each phase is 0.5 for which the bicontinuous morphology, that is necessary for the Siggia's scaling, is more robust. First, we present a few results in the case of the isoviscosity regime and briefly discuss the effects of diffusion and of inertia in this case. Then, the main results of this work, about the effects of symmetry breaking, are presented.

#### A. Symmetric regime

This section is devoted to the determination of the parameters for which the Siggia regime is valid. Indeed, while the three different regimes have been discussed at length in previous work, there is still no clear determination of where the transition occurs. To this purpose, we first give an estimate of the diffusive effects as a function of the  $Pe$  number. Then, we determine the value above which the inertial terms are becoming significant.

To this purpose, we consider various parameter sets for which the Reynolds number and the diffusion process are kept unchanged while the Siggia flow rate is changed. Hence we change the value of the Peclet number without altering either the relative importance of the inertial terms or the absolute value of the diffusive contribution to coarsening owing to the following transformation,

$$v \rightsquigarrow av, \quad (5)$$

$$\rho \rightsquigarrow a^2\rho, \quad (6)$$

where  $a$  is a real constant. Indeed,  $l_0 = v^2/(\gamma\rho)$  (and the Reynolds number) is unchanged while  $v_0 = \gamma/(v\rho)$  is multiplied by  $a$ . More precisely, if a given field  $v(\mathbf{x}, t)$  was a solution of the Navier-Stokes equation, for the original parameter set,  $av(\mathbf{x}, t)$  will be a solution with the transformed parameter set if the diffusive effects are negligible. In this situation, the coarsening rate with the

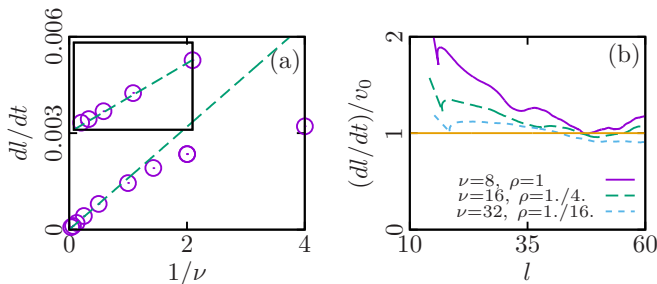


FIG. 2. (a) Growth velocity as a function of viscosity for a volume fraction of 0.5. In the inset, a zoom on the linear regime is shown. (b)  $v/v_0 = dl/dt/v_0$  as a function of  $l$  for  $\rho = 1, 0.25$ , and  $0.0625$  and  $\nu = 8, 16$ , and  $32$ , shown as solid, long, and short dashes, respectively. Here,  $v_0$  is the value computed in the case  $\rho = 0.0625$ ,  $\nu = 32$  (rescaled for  $\rho = 1$  and  $0.25$ ).

transformed parameters will be  $a$  times the coarsening rate with the original parameters, and the relative importance of diffusive effects will be given by the difference between the computed solution and the predicted one. We have applied this approach to our system and the result is presented in Fig. 2(b). The growth velocity multiplied by  $1/v_0$ ,  $0.5/v_0$ , and  $0.25/v_0$  as a function of  $l$  is plotted for  $\nu = 8, 16$ , and  $32$  and  $\rho = 1, 0.25$ , and  $0.0625$ , respectively, where  $v_0$  is the average value of  $dl/dt$  obtained for  $(\nu = 32, \rho = 0.0625)$ . If the diffusive effects are negligible, one expects the curves to collapse, while if diffusive effects are present, the difference between the curves is a measure of the diffusive effects. One can see that the curves obtained for the last two sets of parameters collapse well while for  $\nu = 8$  there is a significant departure from the collapse. As a result, with  $\rho = 1$  and the kinematic viscosity  $\nu < 8$ , diffusion effects can be neglected for values of  $l$  larger than 50. This translates in terms of the Peclet number into the fact that  $Pe > 1$  ( $\gamma = 0.042$ ,  $\rho = 1$ ,  $\nu = 8$ ,  $D = 1 \times A$ , and  $l = 50$ ).

We now turn to the effects of inertia. To this purpose, in Fig. 2(a) we plot the growth velocity of domain size as a function of the inverse of the kinematic viscosity. One can see that, as predicted by Siggia, for high values of  $\nu$  the growth velocity is proportional to  $1/\nu$  with a constant prefactor. For smaller values there is a clear departure from the linear behavior proposed in Ref. [5]. The onset of this deviation occurs for  $\nu \approx 1$  and is significant for  $\nu < 0.5$ , values for which the growth velocity is well described as constant over the length span considered here. As a result, for these values, despite the apparent constant growth rate, there is a clear departure from the Siggia's scaling that is due to inertial effects. From a quantitative point of view, it occurs at  $Re = 1$  ( $\nu = 1$ ,  $\gamma = 0.042$ ,  $\rho = 1$ ,  $l = 25$ ). This value of  $Re = 1$  has to be compared with the one postulated by Siggia that was  $\approx 100$  and that has been widely used since then.

Here, we have characterized the various regimes of domain growth and how they are related. We have also drawn a clear picture of the isoviscous domain growth for a given value of the surface tension ( $\gamma = 0.0042$ ) and the fluid density ( $\rho = 1$ ). For a kinematic viscosity ranging from 4 to 1, and domain sizes ranging from 5 to 100, the growth regime can be described as purely viscous. For lower values of  $\nu$  (corresponding to  $Re \approx 1$ ), a clear departure from this regime due to inertial effects can be seen. For higher values of viscosity (i.e.,  $Pe < 1$ ), the contribution of diffusion to viscosity can no longer be neglected.

### B. Symmetry breaking induced by the viscosity contrast

We now consider the evolution of the microstructure when the two phases have different viscosities. The viscosity contrast ( $VC$ ) is the ratio  $\nu_h/\nu_l$  and ranges from 1 to 128 in our simulations.

First, we consider the evolution of the characteristic length  $l$  when  $\nu_h$  is small enough to guarantee that diffusive effects can be neglected. In such situations, the domain growth over time is linear with a velocity that is a function of both  $\nu_h$  and  $\nu_l$ . In the spirit of Ref. [36], we seek an *effective viscosity*  $\nu_{\text{eff}}$

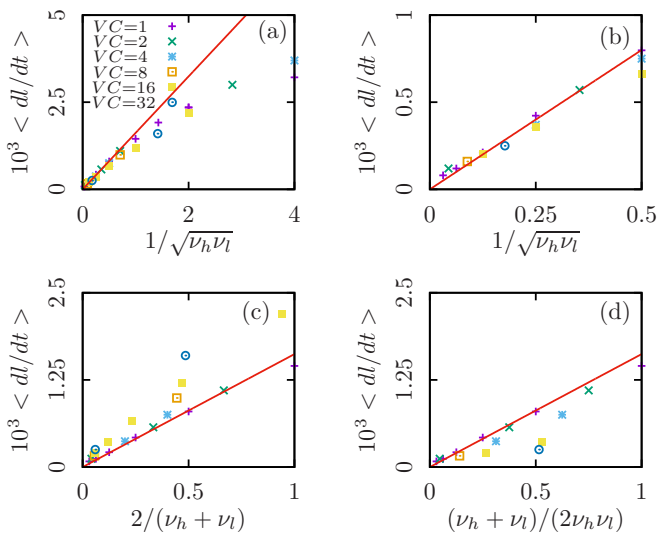


FIG. 3. (a) Growth rate as a function of  $\sqrt{\nu_l \nu_h}$  for different values of  $\nu_h$  ranging from 0.0625 to 32 and of  $\nu_h/\nu_l$  equal to 2, 4, 16, and 32. The points corresponding to  $\nu_h/\nu_l = 1$  are the purple +. The line is a guide to the eye. (b) Same data with a zoom on the vicinity of the origin. (c) and (d) Plot of the coarsening velocity vs (c)  $\nu_{\text{eff}} = (\nu_h + \nu_l)/2$  and (d)  $1/\nu_{\text{eff}} = (1/\nu_h + 1/\nu_l)/2$ .

for the two-phase fluid that predicts the coarsening rate. We consider the following simple forms of the effective viscosity: the arithmetic mean [ $\nu_{\text{eff}} = (\nu_h + \nu_l)/2$ ], the geometric mean ( $\nu_{\text{eff}} = \sqrt{\nu_h \nu_l}$ ), and Onuki's formula [ $1/\nu_{\text{eff}} = (1/\nu_h + 1/\nu_l)/2$ ] [36]. The results are summarized in Fig. 3 and indicate that the use of the geometric mean ( $\sqrt{\nu_h \nu_l}$ ) leads to a very good collapse of the curve giving the coarsening rate as a function of the effective viscosity in the linear regime and still a good collapse when inertial effects are present. Other propositions for the effective viscosity are far less convincing. Hence, the viscous growth of the microstructure is the same as the one that would occur if the viscosity was the geometric mean of the viscosities.

Finally, we describe the effects of the viscosity contrast on the microstructure itself. To this purpose we consider three values of the viscosity contrast (1, 16, and 128) and choose  $\nu_h$  and  $\nu_l$  so that  $\sqrt{\nu_h \nu_l} = 4, 8,$  and  $16$ . To avoid the effect of the diffusive crossover we set the density as  $\rho = 0.00625$ . Using the effective viscosity,  $l_0 \approx 2 \times 10^5$  and the Peclet number is ranging from 5 to 200. Hence we have a set of parameters for which we expect both inertial and diffusive effects to be negligible.

With this parameter set the probability distribution functions (PDFs) of the principal curvatures (rescaled by  $l$ ) are independent of  $\nu_{\text{eff}}$  and of the initial conditions (see Supplemental Material [29]), indicating the generality of the results presented here. In Fig. 4 the contour lines of the PDFs in the two extreme cases ( $VC = 1$  and  $VC = 128$ , with  $\nu_{\text{eff}} = 8$ ) are plotted. As expected in the  $VC = 1$  case, the PDF is symmetric with respect to the axis  $l\kappa_1 = -l\kappa_2$  and the contours corresponding to two times where  $l \approx 23$  and to  $l \approx 84$ , the PDFs are indistinguishable, indicating the self-similar nature of the domain growth. In addition, the contribution of the regions where  $\kappa_1$  is of the same sign as  $\kappa_2$  is negligible.

The self-similar behavior holds in the case  $VC = 128$ , as can be seen in the plot of the structure functions (see Fig. 4), but the plot of the PDF of the curvatures [Fig. 4(b)] is no longer symmetric with respect to the axis  $\kappa_1 = -\kappa_2$ , which clearly indicates the effects of the symmetry breaking. In addition, as for the contribution of the regions where both  $\kappa_1$  and  $\kappa_2 > 0$  are no longer negligible, some regions of the interface between the fluids are spherical caps (as seen in Fig. 1, which was not the case for  $VC = 1$ ). This is also confirmed by the plot of the PDF [Fig. 4(c)] of the Gaussian

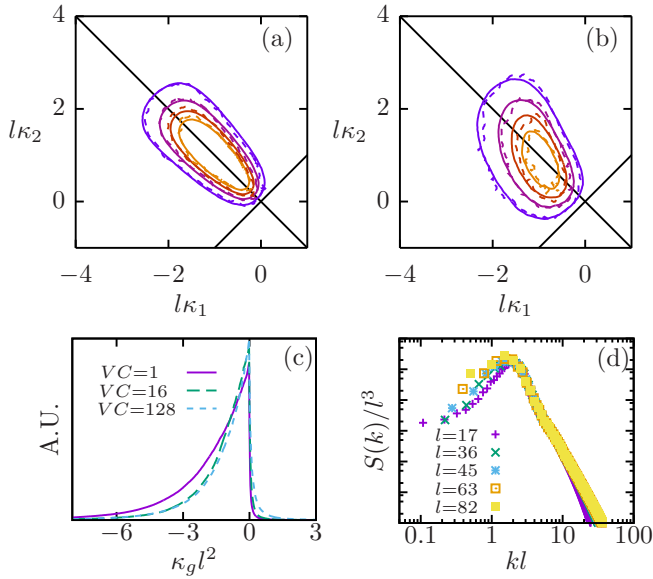


FIG. 4. (a), (b) Contour plots of the PDF of the principal curvatures rescaled by the characteristic length for two values of the viscosity contrast: 1 (128) taken at two times corresponding to (solid)  $l \approx 23$  (30) and to (dashed)  $l \approx 88$  (84) (dashed). The isolevels are 0.0001, 0.0002, 0.0003, 0.0004, and 0.0005. (c) PDF of the Gaussian curvature for three different values of the viscosity contrast (solid: 1; long dashed: 16; and short dashed: 128). (d) Plot of the normalized structure functions taken at different times corresponding to the value of  $l$  indicated on the graph. The very good collapse of the curves for the lowest values of  $l$  confirms the self-similar nature of the coarsening process. The low wave-number departure from the collapse for  $l = 63$  and  $l = 82$  can be attributed to discretization effects [12].

curvature where for viscosity contrasts of 16 and 128, the contribution of the  $\kappa_g > 0$  part of the curve is not negligible, contrary to the  $VC = 1$  case.

Finally, we show the evolution of the rescaled genius number ( $g$ , which is proportional to the rescaled mean Gaussian curvature and a simple function of the Euler's characteristic [29]), and of the rescaled mean curvature ( $\langle l\kappa_m \rangle$ ) as a function of  $l$  for these three values of  $VC$ . After an initial transient, as expected for a self-similar growth, both the genius and the mean curvature are approximately constant for a given value of  $VC$ . In the case of the genius number [Fig. 5(a)], the values computed are similar to the ones found in Ref. [37] ( $\approx 0.13$ ) in the case of diffusive coarsening, and increasing  $VC$  induces a decrease of  $g$ . Nevertheless, the effect is small and there is an increase in measurement error as  $l$  increases. In contrast, the effects on the average mean curvature [Fig. 5(b)]

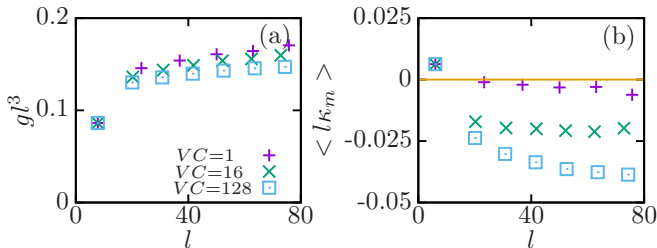


FIG. 5. (a) Plot of the rescaled genius as a function of  $l$  for  $VC = 1$  (+), 16 (x), and 128 (□). (b) Plot of the rescaled average mean curvature as a function of  $l$  for  $VC = 1$  (+), 16 (x), and 128 (□).

are much clearer. Indeed, for  $VC = 1$ , it is 0 (up to numerical/statistical errors) for symmetry reasons. When  $VC$  is increased, there is a clear departure from this value that confirms the symmetry breaking.

The experimental results from Refs. [18,19] give a growth of the Euler characteristic as  $0.98l^{1/3}$  for a  $VC \approx 10^5$  and a volume fraction  $\approx 0.45$  while our results for  $VC = 128$  would correspond to a growth as  $0.7l^{1/3}$ . The difference can be attributed to the dramatic difference in parameter values. From a more qualitative point of view, we find noteworthy the fact that the PDFs of the Gaussian curvature when the viscosity contrast is increased present a significantly higher contribution of  $\kappa_g > 0$ , which corresponds to spherical caps (that are absent in the case  $VC = 1$ ) since in the experiments with high values of  $VC$ , spherical inclusions are observed.

#### IV. CONCLUSION

Here, the hydrodynamical coarsening of a two-phase mixture at symmetric composition is studied using constant and varying viscosity. First, we have challenged the assumption of self-similarity. The analysis of the PDFs of the principal curvatures gives strong arguments in favor of the self-similar nature of the viscous coarsening in both cases. In addition, the analysis presented here is suitable to describe the geometry and topology of the microstructure. More specifically, the effects of the symmetry breaking on the morphology are described and a qualitative agreement with experiments [18,19] is found. When considering the kinetics of the coarsening process, we show that the linear growth regime predicted by Siggia [5] actually exists in the case where the two fluids share the same viscosity for values of the Reynolds number below 1. When symmetry is broken by introducing viscosity contrast, the self-similar linear growth still persists. Furthermore, our analysis allowed us to propose a formula for an effective viscosity that accurately predicts the coarsening rate of the microstructure and may be used to estimate the magnitude of flow-induced coarsening in experiments. This is in contrast with the thoroughly studied case of viscoelastic systems, where a departure from self-similarity is observed [20,24].

Further understanding of the microstructure formation during coarsening should be gained by a study of the pattern formation process in the off-critical mixture  $\phi \neq 0.5$ , where we expect to observe dramatic topological changes during the coarsening process.

#### ACKNOWLEDGMENTS

This work was granted access to the HPC resources of IDRIS under the allocation 2016-A0022B07727 made by GENCI (Grand Équipement National de Calcul Intensif). The authors benefited from the support of the Chaire St-Gobain of École Polytechnique for travel expenses, and was supported by Projects No. K-115959 and No. KKP-126749 of the National Research, Development and Innovation Office (NKFIH), Hungary. Most importantly, they benefited from stimulating discussions with D. Vandembroucq and E. Gouillart.

- 
- [1] A. F. Craievich, J. M. Sanchez, and C. E. Williams, Phase separation and dynamical scaling in borate glasses, *Phys. Rev. B* **34**, 2762 (1986).
  - [2] S. K. Kumar and J. D. Weinhold, Phase Separation in Nearly Symmetric Polymer Mixtures, *Phys. Rev. Lett.* **77**, 1512 (1996).
  - [3] J. W. Cahn, Phase separation by spinodal decomposition in isotropic systems, *J. Chem. Phys.* **42**, 93 (1965).
  - [4] I. M. M. Lifshitz and V. V. Slyozokov, The kinetics of precipitation from supersaturated solutions, *J. Phys. Chem. Solids* **19**, 35 (1961).
  - [5] E. D. Siggia, Late stages of spinodal decomposition in binary mixtures, *Phys. Rev. A* **20**, 595 (1979).
  - [6] Y. Kwon, K. Thornton, and P. W. Voorhees, Coarsening of bicontinuous structures via nonconserved and conserved dynamics, *Phys. Rev. E* **75**, 021120 (2007).

- [7] Y. Kwon, K. Thornton, and P. W. Voorhees, The topology and morphology of bicontinuous interfaces during coarsening, *Europhys. Lett.* **86**, 46005 (2009).
- [8] Y. C. Chou and W. I. Goldburg, Phase separation and coalescence in critically quenched isobutyric-acid and water and 2,6-lutidine water mixtures, *Phys. Rev. A* **20**, 2105 (1979).
- [9] N.-C. Wong and C. M. Knobler, Light-scattering studies of phase separation in isobutyric acid+water mixtures: Hydrodynamic effects, *Phys. Rev. A* **24**, 3205 (1981).
- [10] C. Appert, J. F. Olson, D. H. Rothman, and S. Zaleski, Phase separation in a three-dimensional, two-phase, hydrodynamic lattice gas, *J. Stat. Phys.* **81**, 181 (1995).
- [11] S. Bastea and J. L. Lebowitz, Spinodal Decomposition in Binary Gases, *Phys. Rev. Lett.* **78**, 3499 (1997).
- [12] V. M. Kendon, M. E. Cates, I. Pagonabarraga, J.-C. Desplat, and P. Blandon, Inertial effects in three-dimensional spinodal decomposition of a symmetric binary fluid mixture: A lattice Boltzmann study, *J. Fluid Mech.* **440**, 147 (2001).
- [13] H. Furukawa, Role of inertia in the late stage of the phase separation of a fluid, *Physica A (Amsterdam)* **204**, 237 (1994).
- [14] S. I. Jury, P. Bladon, S. Krishna, and M. E. Cates, Tests of dynamical scaling in three-dimensional spinodal decomposition, *Phys. Rev. E* **59**, R2535 (1999).
- [15] M. Grant and K. R. Elder, Spinodal Decomposition in Fluids, *Phys. Rev. Lett.* **82**, 14 (1999).
- [16] V. M. Kendon, Scaling theory of three-dimensional spinodal turbulence, *Phys. Rev. E* **61**, R6071 (2000).
- [17] A. Sain and M. Grant, Phase Separation of a Binary Fluid in the Inertia-Dominated Regime, *Phys. Rev. Lett.* **95**, 255702 (2005).
- [18] D. Bouttes, E. Gouillart, E. Boller, D. Dalmas, and D. Vandembroucq, Fragmentation and Limits to Dynamical Scaling in Viscous Coarsening: An Interrupted *in situ* X-Ray Tomographic Study, *Phys. Rev. Lett.* **112**, 245701 (2014).
- [19] D. Bouttes, E. Gouillart, and D. Vandembroucq, Topological Symmetry Breaking in Viscous Coarsening, *Phys. Rev. Lett.* **117**, 145702 (2016).
- [20] T. Araki and H. Tanaka, Three-dimensional numerical simulations of viscoelastic phase separation: Morphological characteristics, *Macromolecules* **34**, 1953 (2001).
- [21] J. W. Cahn and J. E. Hilliard, Free energy of a nonuniform system. I. Interfacial free energy, *J. Chem. Phys.* **28**, 258 (1958).
- [22] P. C. Hohenberg and B. I. Halperin, Theory of dynamic critical phenomena, *Rev. Mod. Phys.* **49**, 435 (1977).
- [23] D. M. Anderson, G. B. McFadden, and A. A. Wheeler, Diffuse-interface methods in fluid mechanics, *Annu. Rev. Fluid Mech.* **30**, 139 (1998).
- [24] H. Tanaka, Viscoelastic phase separation, *J. Phys.: Condens. Matter* **12**, R207 (2000).
- [25] S. A. Orszag, Numerical methods for the simulation of turbulence, *Phys. Fluids* **12**, II–250 (1969).
- [26] S. A. Orszag and G. S. Patterson, Numerical Simulation of Three-Dimensional Homogeneous Isotropic Turbulence, *Phys. Rev. Lett.* **28**, 76 (1972).
- [27] C. Liu and J. Shen, A phase field model for the mixture of two incompressible fluids and its approximation by a fourier-spectral method, *Physica D (Amsterdam)* **179**, 211 (2003).
- [28] J. Zhu, L.-Q. Chen, J. Shen, and V. Tikare, Coarsening kinetics from a variable-mobility Cahn-Hilliard equation: Application of a semi-implicit Fourier spectral method, *Phys. Rev. E* **60**, 3564 (1999).
- [29] See Supplemental Material at <http://link.aps.org/supplemental/10.1103/PhysRevFluids.3.074306> for a complete description of the model equation, the numerical method and additional datas.
- [30] B. Z. Shang, N. K. Voulgarakis, and J.-W. Chu, Fluctuating hydrodynamics for multiscale simulation of inhomogeneous fluids: Mapping all-atom molecular dynamics to capillary waves, *J. Chem. Phys.* **135**, 044111 (2011).
- [31] G. I. Tóth, M. Zarifi, and B. Kvamme, Phase-field theory of multicomponent incompressible Cahn-Hilliard liquids, *Phys. Rev. E* **93**, 013126 (2016).
- [32] R. Goldman, Curvature formulas for implicit curves and surfaces, *Comput. Aided Geom. Des.* **22**, 632 (2005).
- [33] J. W. W. Cahn, The later stages of spinodal composition and the beginning of particle coarsening, *Acta Metall.* **14**, 1685 (1966).

- [34] H. Tanaka and T. Araki, Spontaneous Double Phase Separation Induced by Rapid Hydrodynamic Coarsening in Two-Dimensional Fluid Mixtures, [Phys. Rev. Lett.](#) **81**, 389 (1998).
- [35] V. M. Kendon, J.-C. Desplat, P. Bladon, and M. E. Cates, 3D Spinodal Decomposition in the Inertial Regime, [Phys. Rev. Lett.](#) **83**, 576 (1999).
- [36] A. Onuki, Domain growth and rheology in phase-separating binary mixtures with viscosity difference, [Europhys. Lett.](#) **28**, 175 (1994).
- [37] Y. Kwon, K. Thornton, and P. W. Voorhees, Morphology and topology in coarsening of domains via non-conserved and conserved dynamics, [Philos. Mag.](#) **90**, 317 (2010).